On the Performance of Covariance Shaping in Massive MIMO Systems

Placido Mursia, Italo Atzeni, David Gesbert, and Laura Cottatellucci
EURECOM, Communication Systems Department, Sophia Antipolis, France
Emails: {placido.mursia, italo.atzeni, david.gesbert, laura.cottatellucci}@eurecom.fr

***Abstract*—The low-rank behavior of channel covariance matrices in massive multiple-input multiple-output (MIMO) settings can be exploited for pilot decontamination and statistical precoding. In this regard, many well-known algorithms are designed building on the assumption of signal subspace separation among user equipments (UEs), which is hardly satisfied in practice. To cope with this issue, our prior work introduced the concept of *covariance shaping* to enforce statistical orthogonality by exploiting the multiple antennas at the UE-side in the simple case of two UEs. This paper focuses on: *i)* extending the covariance shaping approach to a more general multi-user setting, and *ii)* evaluating its performance in several realistic scenarios, providing useful insights into its behavior and practical implementation.**

***Index Terms*—Covariance shaping, massive MIMO, multi-user MIMO, pilot contamination, statistical beamforming.**

I. Introduction

Massive multiple-input multiple-ouput (MIMO), i.e., a type of multi-user MIMO in which the number of antennas at the base station (BS) is much larger than the number of served user equipments (UEs) [1], is envisioned to be a crucial component of the upcoming 5G standard [2]. Several important works have investigated the role of statistical information in massive MIMO as a means to reduce the complexity of precoding/decoding design as well as the overhead associated with pilot-aided training and feedback of channel state information [3]–[8]. In this regard, a critical aspect of massive MIMO communications is related to the low-rank behavior exhibited by the channel covariance matrices, which is determined by the angle spread spanned by the multipath's angles of arrival (AoAs) at the BS in the case of uniformely-spaced linear arrays [3], [5]. Remarkably, this property allows the BS to distinguish distant UEs with non-overlapping AoAs based on statistical information only. However, perfect separation of the UEs' signal subspaces is very unlikely in practice, as this is dictated by the physical scattering environment and is generally beyond the designer's control.

To cope with this issue, our prior work [9] proposes to exploit the inherent spatial selectivity properties at modern UEs, which are equipped with a small-to-moderate number of antennas, towards a suitable shaping of the channel covariance matrix performed at the UE-side. This approach, referred to as *covariance shaping*, is obtained by means of a statistical beamforming that effectively allows the UEs to excite a suitable subset of all the possible propagation directions towards the BS with the aim of reducing their spatial correlation. In particular, covariance shaping was shown in [9] to successfully enforce partial or full orthogonality between the signal subspaces of two UEs placed close to each other in the context of pilot-contaminated channel estimation [10], outperforming the scenario where the antennas at the UEs are directly used for spatial multiplexing.

In this paper, we analyze in depth the performance of such covariance shaping method in a massive MIMO system. To do so, we firstly extend the work in [9], which focused on the case of two UEs, to a more general multi-user setting. Then, we explore the behavior of such approach in different realistic scenarios, pointing out its effectiveness in separating the channel statistics of different UEs. Finally, we focus on practical implementation aspects of covariance shaping and show substantial performance benefits over a reference scenario where there is no concern for pilot contamination.

This work was supported by the European Research Council under the Horizon 2020 Programme (P. Mursia by MSCA-ITN-ETN 722788 SPOTLIGHT, I. Atzeni and D. Gesbert by ERC-ADG 670896 PERFUME).

II. System Model

A. Channel Model

This paper considers a single-cell multi-user MIMO system where a BS equipped with M antennas serves K UEs equipped with N antennas each. We use $\mathbf{h}_{k,m} \in \mathbb{C}^{N\times 1}$ and $\mathbf{g}_{k,n} \in \mathbb{C}^{1\times M}$ to denote the channel vector between the mth BS antenna and UE k and the channel vector between the BS and the nth antenna of UE k, respectively. The channel matrix between the BS and UE k is thus given by $\mathbf{H}_k \triangleq [\mathbf{h}_{k,1}\dots\mathbf{h}_{k,M}] = [\mathbf{g}_{k,1}^T\dots\mathbf{g}_{k,N}^{\mathrm{T}}]^{\mathrm{T}} \in \mathbb{C}^{N\times M}$. We assume that $\mathrm{vec}(\mathbf{H}_k) \sim \mathcal{CN}(\mathbf{0}, \mathbf{\Sigma}_k)$ [11, Ch.3], where the channel covariance matrix $\mathbf{\Sigma}_k \in \mathbb{C}^{NM\times NM}$ can be written as

$$\mathbf{\Sigma}_k \triangleq \begin{bmatrix} \mathbf{\Sigma}_{k,11} & \mathbf{\Sigma}_{k,12} & \dots & \mathbf{\Sigma}_{k,1M} \\ \mathbf{\Sigma}_{k,12}^{\mathrm{H}} & \mathbf{\Sigma}_{k,22} & & \vdots \\ \vdots & & \ddots & \\ \mathbf{\Sigma}_{k,1M}^{\mathrm{H}} & \dots & & \mathbf{\Sigma}_{k,MM} \end{bmatrix} \tag{1}$$

with $\mathbf{\Sigma}_{k,mn} \triangleq \mathbb{E}[\mathbf{h}_{k,m}\mathbf{h}_{k,n}^{\mathrm{H}}] \in \mathbb{C}^{N\times N}$ being the cross-covariance matrix between the mth and nth columns of $\mathbf{H}_k$. Lastly, the channel covariance matrix seen by UE k is defined as $\mathbf{R}_k \triangleq \mathbb{E}[\mathbf{H}_k\mathbf{H}_k^{\mathrm{H}}] \in \mathbb{C}^{N\times N}$; note that, for the downlink transmission, this represents the receive covariance matrix.

B. Uplink Pilot-Aided Channel Estimation

Assuming a time division duplex (TDD) setting, the channel matrices $\{\mathbf{H}_k\}_{k=1}^K$ are estimated at the BS via uplink pilots. Let $P < K$ denote the number of orthogonal pilots and let $\mathcal{S}_p \triangleq \{k : \text{UE } k \text{ has pilot } p\}$ be the set of UEs that share the same pilot matrix $\mathbf{P}_p \in \mathbb{C}^{N\times\tau}$, with $p = 1, \ldots, P$, where $\{\mathbf{P}_p\mathbf{P}_p^{\mathrm{H}} = \mathbf{I}_N\}_{p=1}^P$ and $\{\mathbf{P}_p\mathbf{P}_q^{\mathrm{H}} = \mathbf{0}\}_{q\neq p}$. We use $\mathbf{Y} \in \mathbb{C}^{M\times\tau}$ to denote the receive signal at the BS during the uplink pilot-aided channel estimation phase, which is given by

$$\mathbf{Y} \triangleq \sqrt{\varrho}\sum_{p=1}^{P}\sum_{k\in\mathcal{S}_p}\mathbf{H}_k^{\mathrm{H}}\mathbf{P}_p + \mathbf{Z} \tag{2}$$

where ϱ is the normalized pilot transmission power and $\mathbf{Z} \in \mathbb{C}^{M\times\tau}$ is the normalized noise at the BS with elements distributed as $\mathcal{CN}(0,1)$. The minimum mean square error (MMSE) estimate of $\mathbf{g}_{k,n}$, with $k \in \mathcal{S}_p$, reads as (see, e.g., [6])

$$\hat{\mathbf{g}}_{k,n}^{\mathrm{H}} \triangleq \frac{1}{\sqrt{\varrho}}\mathbf{\Phi}_{k,nn}\bigg(\sum_{j\in\mathcal{S}_p}\mathbf{\Phi}_{j,nn} + \frac{1}{\varrho}\mathbf{I}_M\bigg)^{-1}\mathbf{Y}\mathbf{P}_p^{\mathrm{H}} \tag{3}$$

where $\mathbf{\Phi}_{k,nn} \triangleq \mathbb{E}[\mathbf{g}_{k,n}^{\mathrm{T}}\mathbf{g}_{k,n}^{*}]$ represents the covariance matrix of $\mathbf{g}_{k,n}$. Finally, the estimate of the channel matrix $\mathbf{H}_k$ is given by $\hat{\mathbf{H}}_k \triangleq [\hat{\mathbf{g}}_{k,1}^{\mathrm{T}} \ldots \hat{\mathbf{g}}_{k,N}^{\mathrm{T}}]^{\mathrm{T}}$.

C. Downlink Data Transmission

Focusing on the downlink data transmission, let $\mathbf{s}_k \in \mathbb{C}^{L_k\times 1}$ denote the data symbol vector corresponding to UE k, with $\mathbb{E}[\mathbf{s}_k\mathbf{s}_k^{\mathrm{H}}] = \mathbf{I}_{L_k}$, and $\mathbf{s} \triangleq [\mathbf{s}_1^{\mathrm{T}} \ldots \mathbf{s}_K^{\mathrm{T}}]^{\mathrm{T}} \in \mathbb{C}^{L\times 1}$, with total number of transmitted symbols given by $L \triangleq \sum_{k=1}^K L_k$. Hence, the signal transmitted by the BS may be written as $\mathbf{x} \triangleq \mathbf{W}\mathbf{s} = \sum_{k=1}^K \mathbf{W}_k\mathbf{s}_k \in \mathbb{C}^{M\times 1}$, where $\mathbf{W} \triangleq [\mathbf{W}_1 \ldots \mathbf{W}_K] \in \mathbb{C}^{M\times L}$ is the multi-user precoding matrix (power constrained as $\|\mathbf{W}\|_{\mathrm{F}}^2 = 1$), where $\mathbf{W}_k \triangleq [\mathbf{w}_{k,1} \ldots \mathbf{w}_{k,L_k}] \in \mathbb{C}^{M\times L_k}$ is the precoding matrix corresponding to $\mathbf{s}_k$. The receive signal at UE k during the downlink data transmission phase is given by

$$\mathbf{y}_k \triangleq \sqrt{\rho}\,\mathbf{H}_k\mathbf{W}_k\mathbf{s}_k + \sqrt{\rho}\sum_{j\neq k}\mathbf{H}_k\mathbf{W}_j\mathbf{s}_j + \mathbf{z}_k \tag{4}$$

where ρ is the normalized transmit power at the BS and $\mathbf{z}_k \sim \mathcal{CN}(\mathbf{0}, \mathbf{I}_N)$ is the normalized noise at UE k. Finally, UE k decodes $\mathbf{s}_k$ as $\hat{\mathbf{s}}_k \triangleq \mathbf{V}_k^{\mathrm{H}}\mathbf{y}_k$, where $\mathbf{V}_k \triangleq [\mathbf{v}_{k,1} \ldots \mathbf{v}_{k,L_k}] \in \mathbb{C}^{N\times L_k}$ is the corresponding combining matrix (power constrained as $\|\mathbf{V}_k\|_{\mathrm{F}}^2 = 1$). The sum rate of such multi-user MIMO system is[1]

$$R \triangleq \sum_{k=1}^{K}\sum_{\ell=1}^{L_k}\log_2\bigg(1+\frac{|\mathbf{v}_{k,\ell}^{\mathrm{H}}\mathbf{H}_k\mathbf{w}_{k,\ell}|^2}{\sum_{j\neq k}|\mathbf{v}_{k,\ell}^{\mathrm{H}}\mathbf{H}_k\mathbf{w}_{j,\ell}|^2 + \rho^{-1}\|\mathbf{v}_{k,\ell}\|^2}\bigg). \tag{5}$$

[1]In Section IV, we use block-diagonalization precoding and MMSE combining for $\mathbf{W}_k$ and $\mathbf{V}_k$, respectively.

III. Covariance Shaping at the UE-Side

Given two UEs k and j, a massive MIMO BS is able to spatially distinguish their channel vectors provided that they exhibit statistical orthogonality. This means that the product of their covariance matrices is the zero matrix, i.e., $\mathbf{\Sigma}_k\mathbf{\Sigma}_j = \mathbf{0}$ [6]. The previos condition occurs when the covariance matrices are rank deficient and share the same eigenbasis. However, such property is rarely satisfied in practice and, in this respect, covariance shaping was proposed in [9] as a means to enforce statistical orthogonality by acting at the UE-side. By preemptively applying statistical beamforming, the UEs aim at reducing interference by separating their channel statistics. Let $\mathbf{v}_k \in \mathbb{C}^{N\times 1}$ be the statistical beamforming vector applied by UE k referred to as the *covariance shaping vector*, whith $\|\mathbf{v}_k\|^2 = 1$. Hence, the corresponding MIMO channel between the BS and each UE k is transformed into an effective multiple-input single-output (MISO) channel, given by $\bar{\mathbf{g}}_k \triangleq \mathbf{v}_k^{\mathrm{H}}\mathbf{H}_k \in \mathbb{C}^{1\times M}$, with $\bar{\mathbf{g}}_k \sim \mathcal{CN}(\mathbf{0}, \bar{\mathbf{\Phi}}_k)$, $\mathbb{E}[\|\bar{\mathbf{g}}_k\|^2] = \mathbf{v}_k^{\mathrm{H}}\mathbf{R}_k\mathbf{v}_k$, and effective channel covariance matrix defined as (see [9] for details)

$$\bar{\mathbf{\Phi}}_k \triangleq \big((\mathbf{I}_M \otimes \mathbf{v}_k^{\mathrm{H}})\mathbf{\Sigma}_k(\mathbf{I}_M \otimes \mathbf{v}_k)\big)^{\mathrm{T}} \tag{6}$$

where the operator $\otimes$ indicates the Kronecker product. The price of such approach is a reduction in the spatial degrees of freedom at the UEs, since the BS can now send only one stream per UE (i.e., $L_k = 1$, $k = 1, \ldots, K$). Note that the spatial multiplexing capability remains at the BS, which can still multiplex one stream per UE.

To estimate the effective channels resulting from covariance shaping, the BS assigns the same pilot vector $\mathbf{p}_p \in \mathbb{C}^{1\times\tau}$ to all UEs $k \in \mathcal{S}_p$, with $\{\|\mathbf{p}_p\|^2 = 1\}_{p=1}^P$ and $\{\mathbf{p}_p\mathbf{p}_q^{\mathrm{H}} = 0\}_{q\neq p}$. We use $\bar{\mathbf{Y}} \in \mathbb{C}^{M\times\tau}$ to denote the receive signal at the BS during the uplink pilot-aided channel estimation phase, which is given by (cf. (2))

$$\bar{\mathbf{Y}} \triangleq \sqrt{\varrho}\sum_{p=1}^{P}\sum_{k\in\mathcal{S}_p}\bar{\mathbf{g}}_k^{\mathrm{H}}\mathbf{p}_p + \mathbf{Z} \tag{7}$$

whereas the MMSE estimate of $\bar{\mathbf{g}}_k$, with $k \in \mathcal{S}_p$, reads as

$$\hat{\bar{\mathbf{g}}}_k^{\mathrm{H}} \triangleq \frac{1}{\sqrt{\varrho}}\bar{\mathbf{\Phi}}_k\bigg(\sum_{j\in\mathcal{S}_p}\bar{\mathbf{\Phi}}_j + \frac{1}{\varrho}\mathbf{I}_M\bigg)^{-1}\bar{\mathbf{Y}}\mathbf{p}_p^{\mathrm{H}}. \tag{8}$$

On the other hand, the receive signal at UE k during the downlink data transmission phase is given by (cf. (4))

$$\bar{y}_k \triangleq \sqrt{\rho}\,\bar{\mathbf{g}}_k\mathbf{w}_k s_k + \sqrt{\rho}\sum_{j\neq k}\bar{\mathbf{g}}_k\mathbf{w}_j s_j + \bar{z}_k \tag{9}$$

with $\bar{z}_k = \mathbf{v}_k^{\mathrm{H}}\mathbf{z}_k \sim \mathcal{CN}(0,1)$, and the resulting sum rate is[2]

$$\bar{R} \triangleq \sum_{k=1}^{K}\log_2\bigg(1+\frac{|\bar{\mathbf{g}}_k\mathbf{w}_k|^2}{\sum_{j\neq k}|\bar{\mathbf{g}}_k\mathbf{w}_j|^2 + \rho^{-1}}\bigg). \tag{10}$$

[2]In Section IV, we assume zero-forcing precoding for $\mathbf{w}_k$.

Since each UE preemptively applies statistical beamforming, there is no need to compute a combining matrix as in Section II-C, thus reducing the related system overhead.

Given the model in [9], two closely spaced UEs k and j attempt to enforce statistical orthogonality between them by applying the covariance shaping vectors $\mathbf{v}_k$ and $\mathbf{v}_j$, respectively. Such vectors can be obtained as the solution to the following optimization problem:

$$\begin{aligned} \min_{\mathbf{v}_k,\mathbf{v}_j} \quad & \frac{\Omega(\mathbf{v}_k,\mathbf{v}_j)}{P_k P_j} \\ \text{s.t.} \quad & \|\mathbf{v}_k\|^2 = \|\mathbf{v}_j\|^2 = 1 \end{aligned} \tag{11}$$

where

$$\Omega(\mathbf{v}_k,\mathbf{v}_j) \triangleq \mathrm{tr}(\bar{\mathbf{\Phi}}_k \bar{\mathbf{\Phi}}_j) \tag{12}$$

$$= \sum_{m,n=1}^{M} \mathbf{v}_k^{\mathrm{H}} \mathbf{\Sigma}_{k,mn} \mathbf{v}_k \mathbf{v}_j^{\mathrm{H}} \mathbf{\Sigma}_{j,nm} \mathbf{v}_j \tag{13}$$

represents a measure of statistical orthogonality between the two UEs and $P_k \triangleq \mathbf{v}_k^{\mathrm{H}} \mathbf{R}_k \mathbf{v}_k$ (resp. $P_j \triangleq \mathbf{v}_j^{\mathrm{H}} \mathbf{R}_j \mathbf{v}_j$) represents the average power transmitted to UE k (resp. to UE j). Problem (11) produces two statistical beamformers that tend to reduce the spatial interaction while preserving the useful power for each UE.

A key point behind covariance shaping lies in exploiting non-Kronecker channel structures. The Kronecker channel model (see, e.g., [12]) describes scenarios in which the channel statistics perceived by transmitter and receiver are independent: this means that it is not possible for any of the two to modify the channel statistics perceived by the other. Such property is typical, for instance, of physical environments where the UE is surrounded by a ring of local scatterers (the so-called one-ring model [3]). In this case, the spatial properties of the channel to the BS cannot be modified by beamforming towards a certain direction due to the proximity of the local scatterers. Hence, under Kronecker channel models, the orthogonality of the channel statistics remains a property of the particular physical environment and cannot be controlled at the UE-side. As a matter of fact, it was shown in [9] that, in this case, the objective of (11) does not depend on the choice of the covariance shaping vectors. For this reason, in the rest of the paper, we assume a non-Kronecker channel structure.

Consider now a generalization of the work in [9] in which the BS is serving K UEs, with $K \geq 2$. Then, for each set $\mathcal{S}_p$, the metric in (11) generalizes to

$$\begin{aligned} \min_{\{\mathbf{v}_k\}_{k\in\mathcal{S}_p}} \quad & \sum_{k\in\mathcal{S}_p} \sum_{j\in\mathcal{S}_p\setminus\{k\}} \frac{\Omega(\mathbf{v}_k,\mathbf{v}_j)}{P_k P_j} \\ \text{s.t.} \quad & \|\mathbf{v}_k\|^2 = 1, \quad \forall k \in \mathcal{S}_p. \end{aligned} \tag{14}$$

Note that the above optimization problem represents the sum of all the possible combinations of (11) for the UEs in each set $\mathcal{S}_p$, where the separation between different sets is ensured by the use of orthogonal pilot sequences. Assuming that the BS has perfect knowledge of the covariance matrices of all UEs,[3] it can solve the P independent optimization problems in (14) (i.e., one for each set $\mathcal{S}_p$) and communicate the resulting covariance shaping vectors to the UEs via proper signaling. Note that such statistical beamformers are re-computed by the BS with the same rate with which the covariance matrices are re-estimated. As proposed in [9], a suboptimal solution for (14) can be efficiently computed via alternate optimization: for each UE $k \in \mathcal{S}_p$, fixing the covariance shaping vector relative to the other UEs $j \in \mathcal{S}_p \setminus \{k\}$, problem (14) reduces to

$$\begin{aligned} \min_{\mathbf{v}_k} \quad & \frac{\mathbf{v}_k^{\mathrm{H}} \mathbf{Q}_k \mathbf{v}_k}{\mathbf{v}_k^{\mathrm{H}} \mathbf{R}_k \mathbf{v}_k} \\ \text{s.t.} \quad & \|\mathbf{v}_k\|^2 = 1, \quad \forall k \in \mathcal{S}_p \end{aligned} \tag{15}$$

where we have defined

$$\mathbf{Q}_k \triangleq \sum_{j\in\mathcal{S}_p\setminus\{k\}} \sum_{m,n=1}^{M} \mathbf{\Sigma}_{k,mn} \eta_{j,mn}^{*} \tag{16}$$

and $\eta_{j,mn}(\mathbf{v}_j) \triangleq \mathbf{v}_j^{\mathrm{H}} \mathbf{\Sigma}_{j,mn} \mathbf{v}_j / (\mathbf{v}_j^{\mathrm{H}} \mathbf{R}_j \mathbf{v}_j)$. Problem (15) is in the form of generalized Rayleigh quotient and its solution corresponds to the minimum eigenvector of $\mathbf{R}_k^{-1}\mathbf{Q}_k$. A similar optimization problem is obtained for the other UEs, and the procedure is repeated until convergence is reached, i.e., until the covariance shaping vectors do not change substantially over consecutive iterations.

IV. Performance Evaluation

In this section, we present numerical results to evaluate the performance gains of the covariance shaping method at the UE-side. We thus compare the following two scenarios:

1) **Reference scenario.** The BS estimates the MIMO channels $\{\mathbf{H}_k\}_{k=1}^K$ using $P < K$ orthogonal pilot sequences during the uplink training phase and obtains the corresponding estimates $\{\hat{\mathbf{H}}_k\}_{k=1}^K$ as described in Section II-B. In the downlink data transmission phase, the BS adopts block-diagonalization precoding on the estimated channels [13]. Assuming that each UE k has perfect knowledge of both the estimated channel $\hat{\mathbf{H}}_k$ available at the BS and its corresponding precoding matrix $\mathbf{W}_k$, it applies the MMSE combining matrix[4]

$$\mathbf{V}_k = \frac{\left(\hat{\mathbf{H}}_k \mathbf{W}_k \mathbf{W}_k^{\mathrm{H}} \hat{\mathbf{H}}_k^{\mathrm{H}} + \frac{1}{\rho}\mathbf{I}_N\right)^{-1} \hat{\mathbf{H}}_k \mathbf{W}_k}{\left\| \left(\hat{\mathbf{H}}_k \mathbf{W}_k \mathbf{W}_k^{\mathrm{H}} \hat{\mathbf{H}}_k^{\mathrm{H}} + \frac{1}{\rho}\mathbf{I}_N\right)^{-1} \hat{\mathbf{H}}_k \mathbf{W}_k \right\|_{\mathrm{F}}}. \tag{17}$$

2) **Covariance shaping scenario.** The BS computes the covariance shaping vectors and communicates to each UE k its corresponding $\mathbf{v}_k$ on a separate feedback channel. Then, the BS estimates the effective MISO channels $\{\bar{\mathbf{g}}_k\}_{k=1}^K$ resulting from covariance shaping using $P < K$ orthogonal pilot sequences during the uplink training phase and obtains the corresponding

[3] Note that this is a reasonable assumption due to the long-term validity of the channel statistics.

[4] Note that this implies extra communication resources to feed back this information to the UE. Moreover, we neglect the possible further degradation in the estimated channels fed back by the BS to the UEs.

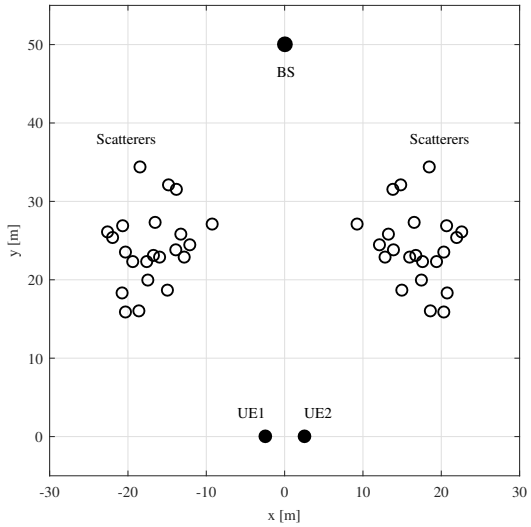

Figure 1. Position of the BS, UEs, and scatterers in the LoS scenario.

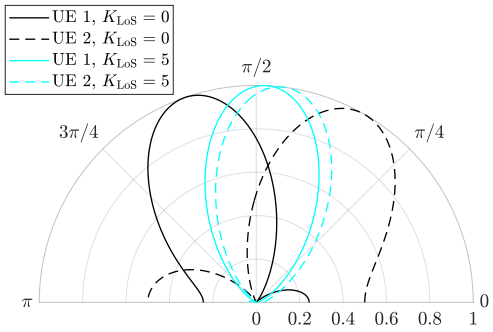

Figure 2. Antenna diagram of the covariance shaping vectors at the UE-side obtained solving (14), with $N = 2$ and for different values of the Rice factor K_{LoS}.

estimates $\hat{\tilde{\mathbf{g}}}_k$ as described in Section III. In the downlink data transmission phase, the BS adopts zero-forcing precoding on the estimated channels, i.e.,

$$\mathbf{W} = \frac{\hat{\tilde{\mathbf{H}}}^{\mathrm{H}}(\hat{\tilde{\mathbf{H}}}\hat{\tilde{\mathbf{H}}}^{\mathrm{H}})^{-1}}{\|\hat{\tilde{\mathbf{H}}}^{\mathrm{H}}(\hat{\tilde{\mathbf{H}}}\hat{\tilde{\mathbf{H}}}^{\mathrm{H}})^{-1}\|_{\mathrm{F}}} \tag{18}$$

where we have defined $\hat{\tilde{\mathbf{H}}} \triangleq [\hat{\tilde{\mathbf{g}}}_1^{\mathrm{T}} \dots \hat{\tilde{\mathbf{g}}}_K^{\mathrm{T}}]^{\mathrm{T}}$.

We consider a propagation environment consisting of a line-of-sight (LoS) path and a set of scattered paths between the BS and the UEs. The expression of $\mathbf{H}_k$ follows the *discrete physical channel model* (see, e.g., [14]) with both LoS and scattered components. Let $\mathbf{a}(\theta) \in \mathbb{C}^{N\times 1}$ and $\mathbf{b}(\phi) \in \mathbb{C}^{M\times 1}$ denote the uniform linear array responses of UE k and of the BS defined as

$$\mathbf{a}(\theta) \triangleq \frac{1}{\sqrt{N}}[1\, e^{-2\pi\delta\sin(\theta)} \dots e^{-2\pi(N-1)\delta\sin(\theta)}]^{\mathrm{T}}, \tag{19}$$

$$\mathbf{b}(\phi) \triangleq \frac{1}{\sqrt{M}}[1\, e^{-2\pi\delta\sin(\phi)} \dots e^{-2\pi(M-1)\delta\sin(\phi)}]^{\mathrm{T}} \tag{20}$$

respectively, where δ is the ratio between the antenna spacing and the signal wavelength. Using K_{LoS} to denote the ratio

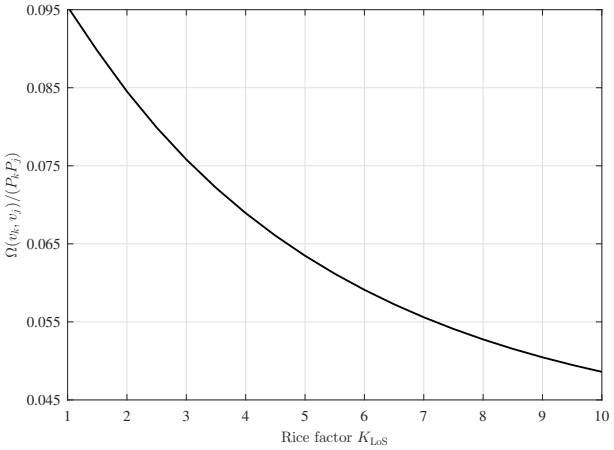

Figure 3. Optimized metric in (11) versus the Rice factor K_{LoS}, with $M = 64$, $N = 2$, and $K = 2$.

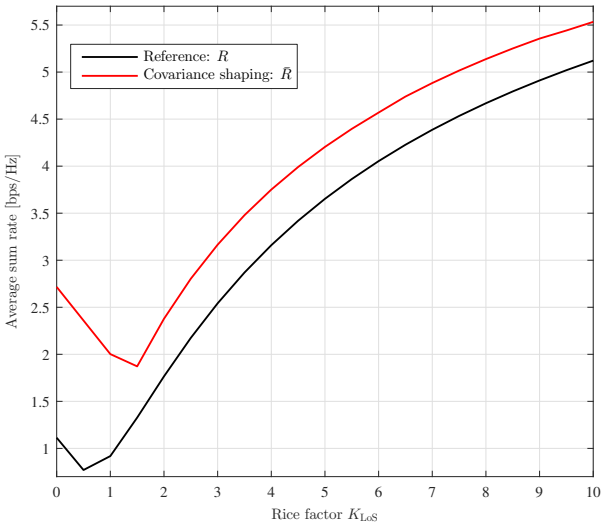

Figure 4. Average sum rate of the reference and the covariance shaping scenario versus the Rice factor K_{LoS}, with $M = 64$, $N = 2$, $K = 2$, and receive SNR at the UEs of 20 dB.

between the power of the LoS path and any scattered path, the channel matrix between the BS and UE k is given by

$$\mathbf{H}_k = \sqrt{\frac{K_{\text{LoS}}}{K_{\text{LoS}}+1}}\frac{\alpha_{k,\text{LoS}}}{d_{k,\text{LoS}}^{\beta/2}}\mathbf{a}(\theta_{k,\text{LoS}})\mathbf{b}^{\mathrm{H}}(\phi_{k,\text{LoS}}) + \sqrt{\frac{1}{K_{\text{LoS}}+1}}\sum_{u=1}^{U}\frac{\alpha_{k,u}}{d_{k,u}^{\beta/2}}\mathbf{a}(\theta_{k,u})\mathbf{b}^{\mathrm{H}}(\phi_{k,u}) \tag{21}$$

where U is the total number of scattered paths, $\alpha_{k,u}$ (resp. $\alpha_{k,\text{LoS}}$) is the random phase delay for the scattered path u (resp. for the LoS path), $d_{k,u}$ (resp. $d_{k,\text{LoS}}$) is the distance of the scattered path u (resp. of the LoS path), $\beta = 2$ is the pathloss exponent, while $\theta_{k,u}$ and $\phi_{k,u}$ (resp. $\theta_{k,\text{LoS}}$ and $\phi_{k,\text{LoS}}$) are the angles of impingement of the scattered path u (resp. of the LoS path) on the antenna array of UE k and the BS, respectively. Lastly, we consider $N = 2$ antennas at

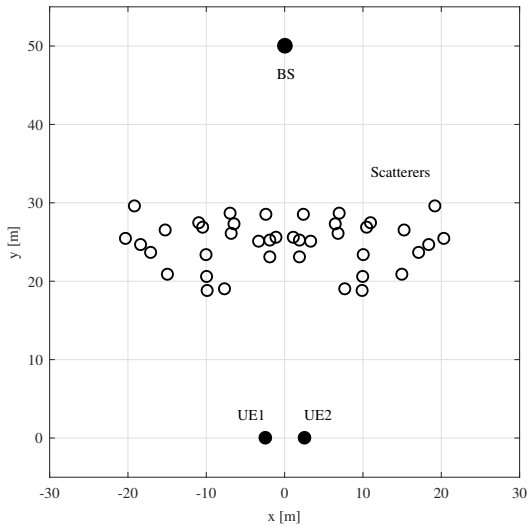

Figure 5. Position of the BS, UEs, and scatterers in the NLoS scenario.

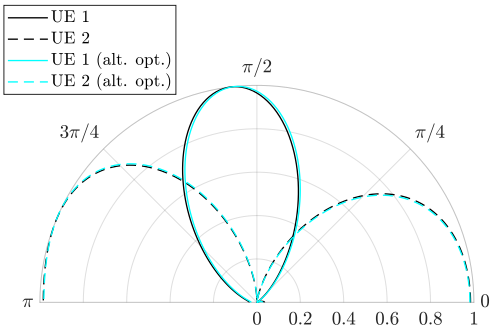

Figure 6. Antenna diagram of the covariance shaping vectors at the UE-side obtained solving (14) and (15) (alternate optimization) in the NLoS scenario, with $N = 2$.

the UEs and, unless otherwise stated, $M = 64$ antennas at the BS.

A. Two-UE Setting

In this section we firstly focus on the case of $K = 2$ UEs in order to better present the key characteristics of the proposed covariance shaping method. In particular, we analyze the impact of the physical scattering environment as well as the number of BS antennas M. Indeed, the solution to (14) and (15) depends only on channel statistics and, hence, on the physical scattering environment. Thus, the solution to these problems is to beamform along directions that trade off between preserving the useful power and enforcing statistical orthogonality. Consider first the scenario shown in Figure 1, referred to as *LoS scenario*, where a set of scatterers are randomly placed within two separate clusters, creating three macro channel directions, i.e., the two sets of scattered paths and the LoS path. In this setting, the latter carries generally more power than any other scattered path and thus represents a relatively strong channel direction. As a result, the covariance shaping might be less effective in enforcing

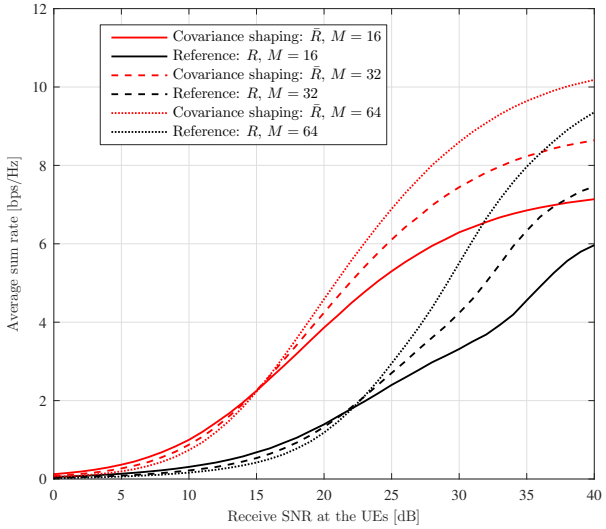

Figure 7. Average sum rate of the reference and the covariance shaping scenario versus receive SNR at the UEs with $N = 2$, $K = 2$, and for different values of M.

statistical orthogonality, since the beamformers will deviate only slightly from the LoS to avoid an excessive loss of power. Such comparison is depicted in Figure 2 where, as the Rice factor K_{LoS} increases, the antenna diagram of the covariance shaping vectors for two closely spaced UEs tend to align towards the LoS direction. In addition, Figure 3 shows the solution to problem (11) versus the Rice factor, where the monotonically decreasing trend results from the increasing power received by the UEs through the LoS path. In Figure 4, the average sum rate of the covariance shaping approach versus the reference scenario is shown assuming receive signal-to-noise ratio (SNR) of 20 dB. As the Rice factor increases, the two curves get closer since the covariance shaping is less effective in restoring orthogonality. On the contrary, consider the scenario in Figure 5, referred to as *NLoS scenario*, where the LoS path is absent, obstructed by a set of randomly placed scatterers: in this setting the covariance shaping vectors select nearly orthogonal channel directions, as shown in Figure 6. Lastly, Figure 7 shows how covariance shaping is more effective as the number of antennas at the BS increases. This is due to the enhanced spatial resolution at the BS-side.

B. General Multi-User Setting

In this section, we evaluate the performance of the proposed covariance shaping method in a multi-user MIMO scenario, with $K \geq 2$. To do so, by assuming that the BS has an estimate of the position of each UE (see, for instance, [15]), we divide the K UEs into the P sets $\{\mathcal{S}_p\}_{p=1}^{P}$ via the following two alternative clustering strategies (CSs), as shown in Figure 8:

1) **Clustering strategy 1 (CS 1).** The clusters are formed via the K-means clustering algorithm in order to partition the UEs in P spatially disjoint sets.

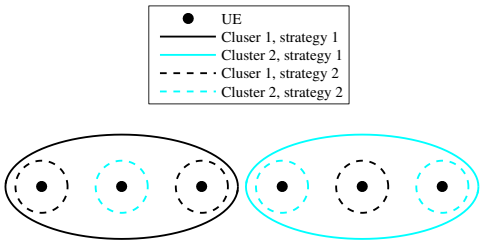

Figure 8. Proposed clustering strategies, with $K = 6$ and $P = 2$.

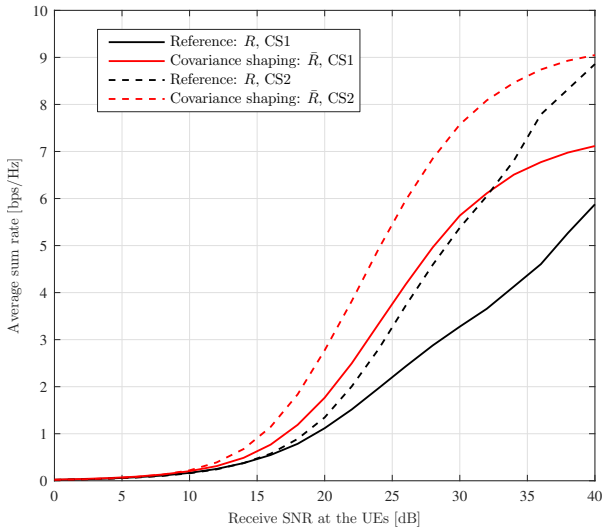

Figure 9. Average sum rate of the reference and the covariance shaping scenario versus receive SNR at the UEs, with $M = 64$, $N = 2$, $P = 2$, $K = 6$, $K_{\text{LoS}} = 2$, and for the two different CSs for pilot assignment.

2) **Clustering strategy 2 (CS 2).** The UEs are divided into P clusters by maximizing the sum distance between all pairs of UEs in the same cluster.

Hence, covariance shaping is applied independently per-cluster and inter-cluster separation is ensured by the use of orthogonal pilots. The scenario taken into consideration includes of $K = 6$ closely spaced UEs divided into $P = 2$ clusters in the presence of a LoS, as in Figure 1, with Rice factor $K_{\text{LoS}} = 2$. Figure 9 shows the average sum rate for the reference and covariance shaping scenarios versus the receive SNR at the UEs, assuming that the latter is the same as the SNR at the BS during the uplink training phase. The enhanced performance of covariance shaping stems from substantially less pilot-contaminated channel estimates, which result in more efficient downlink precoding. Indeed, the latter takes advantage of both superior quality of channel estimates and statistical spatial separation enforced by the UEs with their covariance shaping vectors. The block diagonalization in the reference scenario tends instead to cancel both interfering and useful channels due to severely interference-limited channel estimates. In addition, CS 2 outperforms CS 1 over the whole SNR range, given that the UEs in each cluster have higher relative distance, which results in more effective covariance shaping.

V. Conclusions

This paper further investigates covariance shaping for massive MIMO systems, which was proposed in our prior work [9], and numerically evaluates its performance in a general multi-user MIMO setting. In this respect, multi-antenna UEs are divided into clusters sharing the same pilot sequence and attempt to enforce intra-cluster statistical orthogonality by means of a suitably designed statistical beamformer. Assuming perfect knowledge of the channel statistics, the BS can assign both the pilot sequences and the covariance shaping vectors to the UEs. The price for such approach is a reduction in the spatial degrees of freedom at the UEs. We apply covariance shaping in several realistic scenarios, providing insights into its behavior and practical implementation. Numerical results show that this method outperforms a reference scenario where the multiple antennas at the UEs are used for spatial multiplexing only, without concern for pilot contamination.

References

[1] T. L. Marzetta, "Noncooperative cellular wireless with unlimited numbers of base station antennas," *IEEE Trans. Wireless Commun.*, vol. 9, no. 11, pp. 3590–3600, Nov. 2010.

[2] J. G. Andrews, S. Buzzi, W. Choi, S. V. Hanly, A. Lozano, A. C. K. Soong, and J. C. Zhang, "What will 5G be?" *IEEE J. Sel. Areas Commun.*, vol. 32, no. 6, pp. 1065–1082, June 2014.

[3] H. Yin, D. Gesbert, M. Filippou, and Y. Liu, "A coordinated approach to channel estimation in large-scale multiple-antenna systems," *IEEE J. Sel. Areas Commun.*, vol. 31, no. 2, pp. 264–273, Feb. 2013.

[4] H. Yin, D. Gesbert, and L. Cottatellucci, "Dealing with interference in distributed large-scale MIMO systems: A statistical approach," *IEEE J. Sel. Topics Signal Process.*, vol. 8, no. 5, pp. 942–953, Oct. 2014.

[5] J. Nam, A. Adhikary, J. Y. Ahn, and G. Caire, "Joint spatial division and multiplexing: Opportunistic beamforming, user grouping and simplified downlink scheduling," *IEEE J. Sel. Topics Signal Process.*, vol. 8, no. 5, pp. 876–890, Oct. 2014.

[6] E. Björnson, J. Hoydis, and L. Sanguinetti, "Massive MIMO has unlimited capacity," *IEEE Trans. Wireless Commun.*, vol. 17, no. 1, pp. 574–590, Jan. 2018.

[7] R. Müller, L. Cottatellucci, and M. Vehkaperä, "Blind pilot decontamination," *IEEE J. Sel. Topics Signal Process.*, vol. 8, no. 5, pp. 773–786, Oct. 2014.

[8] L. You, X. Gao, X. Xia, N. Ma, and Y. Peng, "Pilot reuse for massive MIMO transmission over spatially correlated Rayleigh fading channels," *IEEE Trans. Wireless Commun.*, vol. 14, no. 6, pp. 3352–3366, June 2015.

[9] P. Mursia, I. Atzeni, D. Gesbert, and L. Cottatellucci, "Covariance shaping for massive MIMO systems," in *Proc. IEEE Global Commun. Conf. (GLOBECOM)*, Abu Dhabi, UAE, Dec. 2018.

[10] J. Jose, A. Ashikhmin, T. L. Marzetta, and S. Vishwanath, "Pilot contamination and precoding in multi-cell TDD systems," *IEEE Trans. Wireless Commun.*, vol. 10, no. 8, pp. 2640–2651, Aug. 2011.

[11] A. Paulraj, R. Nabar, and D. Gore, *Introduction to Space-Time Wireless Communications*, 1st ed. New York, NY, USA: Cambridge University Press, 2008.

[12] J. P. Kermoal, L. Schumacher, K. I. Pedersen, P. E. Mogensen, and F. Frederiksen, "A stochastic MIMO radio channel model with experimental validation," *IEEE J. Sel. Areas Commun.*, vol. 20, no. 6, pp. 1211–1226, Aug. 2002.

[13] Q. H. Spencer, A. L. Swindlehurst, and M. Haardt, "Zero-forcing methods for downlink spatial multiplexing in multiuser MIMO channels," *IEEE Trans. Signal Process.*, vol. 52, no. 2, pp. 461–471, Feb. 2004.

[14] A. M. Sayeed, "Deconstructing multiantenna fading channels," *IEEE Trans. Signal Process.*, vol. 50, no. 10, pp. 2563–2579, Oct. 2002.

[15] D. Xenakis, L. Merakos, M. Kountouris, N. Passas, and C. Verikoukis, "Distance distributions and proximity estimation given knowledge of the heterogeneous network layout," *IEEE Trans. Wireless Commun.*, vol. 14, no. 10, pp. 5498–5512, Oct. 2015.